



ISSN: 0067-2904

## Topsoil Magnetic Susceptibility and Heavy Metal Contamination: A Case Study in Al-Muthanna Province, Iraq

**Nawrass Ameen**

College of Education for Pure Science, University of Al Muthanna, 66001 Samawa, Iraq

Received: 26/6/ 2019

Accepted: 24/ 8/2019

### Abstract

Due to rapid urbanization and industrialization that occurred in Al- Muthanna province in southeastern Iraq during the last decade, pollutants such as heavy metals were emitted into the environment and became a serious threat to human health. Environmental pollution could be caused by different types of pollutants, which come from different sources.

This study aims to assess the environmental magnetism efficiency for heavy metal pollution assessment using the magnetic susceptibility technique which became a more rapid and cost-effective compared to conventional methods. Increasing heavy metal contents in soils causes an increase in the magnetic mineral concentration. The study area is located in Al- Muthanna province, southeast of Iraq, and contains three cement plants, an oil refinery, bricks factories, and power plants. Fifty topsoil and subsoil samples (0-50 cm depth) were collected from five sites; Al- Jinoob cement plant (one site), Samawa oil refinery (two sites) and Al- Muthanna cement plant (two sites). In this study, magnetic properties of samples in vertical sections and levels of heavy metal elements; of selected samples from regions with different geological settings were compared. The heavy metals analysis included chromium (Cu), iron (Fe), nickel (Ni), copper (Cu), Arsenic (As) and lead (Pb), which could give indications of heavy metal pollution in soil. The highest magnetic susceptibility value ( $65.23 \times 10^{-8} \text{ m}^3 \text{ kg}^{-1}$ ) was recorded in Al-Muthanna cement plant (TSL-4) and the highest Cu concentration (602.57 ppm) was also recorded in Al-Muthanna cement plant (TSL-5-3). The results of magnetic properties show the dominance of coarse magnetite, which is supposed to have originated from pedogenic particles in natural soils, causing the positive correlation between magnetic susceptibility ( $\chi$ ) and anhysteretic remanent magnetisation (ARM). According to the results of frequency dependent susceptibility ratio ( $\kappa_{fd}\%$ ), the magnetic particles showed an admixture of multi-domain and pseudo-single domain behaviour. Magnetic susceptibility and heavy metal analyses results indicated emissions from nearby industrial plants. X-ray fluorescence (XRF) was carried out for heavy metal analyses which supported our results. Results of this study demonstrate the suitability of applying magnetic techniques for assessing environmental situations.

**Keywords:** Magnetic susceptibility, Topsoil, Heavy metals, Environmental pollution

الحساسية المغناطيسية للتربة السطحية وتلوث العناصر الثقيلة: دراسة في محافظة المثنى، العراق

نورس ناهض امين

كلية التربية للعلوم الصرفة، جامعة المثنى، المثنى، العراق

## الخلاصة

نظراً للتحضر السريع والتصنيع الذي حدث في محافظة المثنى في جنوب شرق العراق خلال العقد الماضي، فإن الملوثات مثل المعادن الثقيلة انبعثت في البيئة وأصبحت ذات تهديداً خطيراً على صحة الإنسان. ان التلوث البيئي قد يحدث من انواع مختلفة من الملوثات والتي تأتي من مصادر مختلفة. تهدف هذه الدراسة إلى تقييم كفاءة الطريقة لمغناطيسية البيئية لتقييم تلوث التربة بالمعادن الثقيلة باستخدام تقنية الحساسية المغناطيسية والتي اصبحت طريقة سريعة وفعالة من حيث التكلفة مقارنة بالطرق التقليدية. ان ارتفاع محتوى التربة من العناصر الثقيلة سيزيد من تركيز المعادن المغناطيسية. تقع منطقة الدراسة في محافظة المثنى ، جنوب شرق العراق ، والتي تحتوي على ثلاثة مصانع للأسمنت ومصفاة للنفط ومصانع الطابوق ومحطات الطاقة. تم جمع خمسين عينة من التربة السطحية و تحت السطحية (0-50 سم) من خمسة مواقع ؛ مصنع اسمنت الجنوب (موقع واحد) ، مصفاة السماوة (موقعين) ومصنع اسمنت المثنى (موقعين). في هذه الدراسة ، تمت مقارنة الخواص المغناطيسية للعينات في المقاطع الرأسية والعناصر المعدنية الثقيلة (الكروم ، الحديد ، النيكل ، النحاس ، القصدير، الرصاص) (والتي تعطي مؤشر على تلوث التربة بالعناصر الثقيلة) لعينات مختارة من المناطق ذات جيولوجية مختلفة. سجلت اعلى قيمة للحساسية المغناطيسية في منطقة معمل اسمنت المثنى ( $65.23 \times 10^{-8} \text{ m}^3\text{kg}^{-1}$ ) (TSL-4) واعلى قيمة لعنصر النحاس (602.57 ppm) كانت ايضاً ضمن موقع معمل اسمنت المثنى (TSL-5-3).

اظهرت النتائج المغناطيسية سيادة حبيبات معدن المغناطيت الكبيرة والتي من المفترض أنها قد نشأت من جزينات متجانسة في التربة الطبيعية مما تسبب في وجود علاقة إيجابية بين قيمة الحساسية المغناطيسية  $\chi$  وقيم المغناطيسية المتبقية (ARM). وفقاً لنتائج الحساسية التي تعتمد على التردد ( $K_{fd}$  %)، تُظهر الحبيبات المغناطيسية مزيجاً من حبيبات مغناطيسية (متعدد الانطقة) و حبيبات ذات نطاق واحد. تشير نتائج تحليل الحساسية المغناطيسية والمعادن الثقيلة إلى ان تلوث التربة ناتج عن انبعاثات العناصر الثقيلة من المنشآت الصناعية القريبة. ان نتائج تحليل الأشعة السينية (XRF) لتحليل المعادن الثقيلة دعمت نتائجنا. توضح نتائج هذه الدراسة مدى ملائمة تطبيق التقنيات المغناطيسية لتقييم الوضع البيئي.

## Introduction

Industrial processes related to anthropogenic activities increase pollution rates and give rise to dangerous particle emission, including different magnetic minerals. After the particles are settled down in soils, they penetrate through the subsoils and sediments reaching to groundwater. Various studies were conducted to discriminate the magnetic mineralogy and heavy metal concentrations and to draw correlations between them.

A previous work [1] studied the magnetic susceptibility and heavy metal contamination in agricultural soils and concluded that they were highly recorded, positively correlated, and strongly influenced by anthropogenic activities.

In some cases, the presence of heavy metals in the topsoil can be regarded as an indication of inorganic soil contamination, as identified by magnetic measurements [2]. Presence of heavy metals is connected with magnetic particles, which are magnetic signal carriers in atmospheric dust. This was concluded from a study performed in alkaline dusts from power and cement plants in southern Poland [2].

A rock magnetic study was conducted for lake sediments in southern Iraq [3] and the results showed the dominance of hard magnetic (hematite) and soft magnetic (magnetite) phases (as the main magnetic carriers) along with a small portion of super-paramagnetic particles. Improved magnetic measurements could be used as a proxy measure for the degree of heavy metal contamination, showing the distribution of pollution components in industrial sectors and indicating powerful anthropogenic contribution in soil samples [4].

A combined assessment of the concentration, type, and mineral grain size of magnetic minerals in road dust samples could identify the sources of pollutants in road dust, while magnetic measurements were widely used as prospective tools to monitor and classify pollution [5]. The high value of

magnetic mineral content in road dust is dispersed largely in regions with more demand for building materials, greater housing density, and heavier traffic than anywhere else in the region.

The research presented in this work is focused on an intense pollution area; Samawa City (Al-Muthanna province) with population of about 700.000 which had two cement plants, one oil refinery and many brick factories. These anthropogenic activities are a main factor in increasing the emissions of heavy metal particles, which settle on the soils and affect the vegetation and human health. This study aimed at a comprehensive description of the mineral particles of dust from the above-mentioned pollution sources, with special respect to the magnetic minerals detection by magnetic measurements of this dust as the main carrier of heavy metals. The method of magnetic mineralogy was used to assess the heavy metal content and test the use of magnetic susceptibility as proxy measurement.

## Materials and methods

### 1. Site description

The study area is located in Samawa City, Al-Muthanna province, south-western Iraq (Figure-1). The governorate's landscape is dominated by desert plains, with only a small ribbon of irrigated agricultural land in the north along the Euphrates River. The climate in Al-Muthanna is a dry desert, with temperatures easily exceed 40 °C during the summer, while rainfall is very scarce and limited to the winter months. The direction of the wind is northwest.

The geological settings of Samawa City is generally flat and covered by 1-10 m of recent alluvial deposits, which unconformably overlie three formations identified by paleontological and lithological studies. The three formations are, from bottom to top: (1) the Rus Formation, consisting of more than 90 m of anhydrite rocks alternating with thin beds of nonfossiliferous limestone and marl; (2) the Dammam Formation, consisting of limestone and dolomitic limestone and dolomite and (3) the Euphrates Formation, consisting of conglomerate, marl and limestone [6].

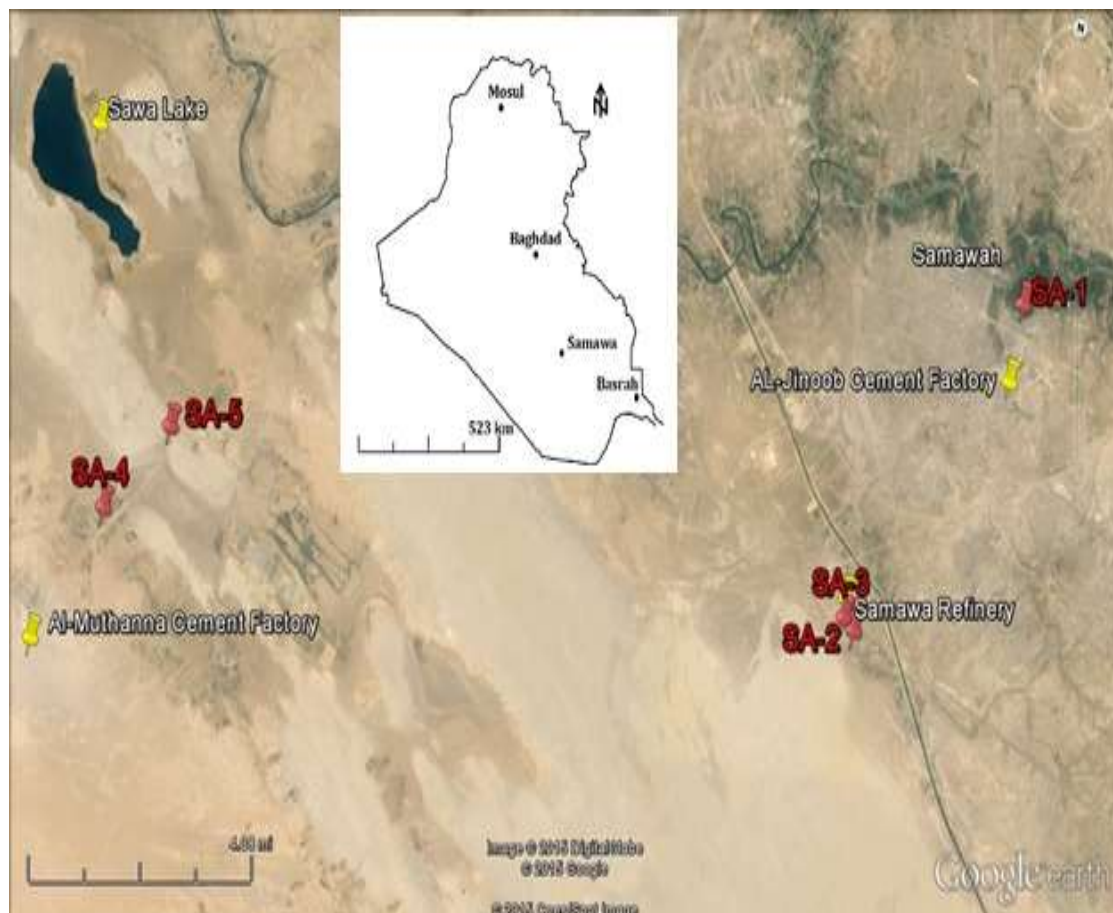


**Figure 1**-Location map of the five sampling sites; Al-Jinoob cement plant (SA-1), Samawa oil refinery (SA-2, SA-3) and Al-Muthanna cement plant (SA-4, SA-5).

## 2. Field work

Fifty topsoil and subsoil samples (vertical profiles) of 0-50 cm depth were carefully collected as one sample for each 5 cm to obtain better resolution and to cover different industrial areas from five sites; Al-Jinoob cement plant (one site), Samawa oil refinery (two sites) and Al-Muthanna cement plant (two sites).

The samples were put in sealable plastic bags of pocket size, tagged, permitted to be air dried at room temperature, and then transferred for magnetic measurements to the magnetic laboratory at Tübingen University, Germany.

## 3. Experimental Methods

### 3.1 Magnetic monitoring

After air drying in the laboratory, the 5 cm-interval samples were homogenized and about 17 g of subsoil samples were packed into 10 cm<sup>3</sup> nonmagnetic cylindrical plastic boxes for the following series of magnetic measurements; bulk magnetic susceptibility ( $\kappa$ ) of soil samples was measured with a Kappabridge Kly-3 (AGICO) and normalized to the mass, determining the mass-specific magnetic susceptibility ( $\chi$ ). Frequency-dependent magnetic susceptibility was measured with a Kappabridge MFK1-FA at two different frequencies of 976 Hz and 15.616 Hz in a peak field of 200 A/m, then  $\kappa_{fd}\%$  was calculated ( $\kappa_{fd}\% = (\kappa_{lf} - \kappa_{hf})/\kappa_{lf} \times 100$ ). This parameter is sensitive to the presence of ultrafine super-paramagnetic magnetite grains [7]. Anhysteretic remanent magnetization (ARM) was measured by a long-core cryogenic magnetometer (2G Enterprises Model 755-1.65UC). MMPM9 pulse magnetizer (Magnetic Measurements Ltd.) was used and the S-ratio was calculated using a saturated isothermal remanent magnetization (SIRM) of the samples with a maximum field (1 T) for the SIRM and a reverse field IRM of 0.3 T (IRM-300) based on a previously reported equation [8]. A CS-3 heating device attached to the Kappabridge KLY-3 (AGICO) was used to perform thermomagnetic runs of magnetic susceptibility ( $\kappa$ -T) from room temperature to 700 °C. All magnetic and grain size measurements were carried out in the magnetic laboratories at the Department of Geosciences, University of Tübingen.

### 3.2 X-ray fluorescence

Analysis of X-ray fluorescence (XRF) was used to explore the selected samples for heavy metal content of Cr, Fe, Ni, Cu, As, Pb; the samples were grinded and then analyzed with the Ametek Spectro Xepos model Xepos 03 9STD Gas in the German- Iraqi laboratory at the Geology Department, University of Baghdad, Iraq.

### 3.3 Grain size analyses

For selected samples, Laser-beam diffraction coupled with a Malvern Mastersizer 2000 which is sensitive to particle diameters between 20 nm to 2 mm, were used to measure the bulk grain size distribution. Then the grain size was determined (after removal of organic matter and dissolution of carbonate). Statistical analysis was implemented to assess the results.

## Results and Discussion

Vertical profiles of mass-specific magnetic susceptibility for the five sites are shown in Figure-2.  $\chi$  decreased with depth in the five sites; in Al-Jinoob cement plant (TSL1), magnetic susceptibilities varied from 14.04 to 32.72  $\times 10^{-8} \text{ m}^3\text{kg}^{-1}$  with a mean value of 25.74  $\times 10^{-8} \text{ m}^3\text{kg}^{-1}$ , whereas the magnetic susceptibility values varied between 13.29 to 63.15  $\times 10^{-8} \text{ m}^3\text{kg}^{-1}$  with a mean value of 35.82  $\times 10^{-8} \text{ m}^3\text{kg}^{-1}$  and 16.17 to 36.60  $\times 10^{-8} \text{ m}^3\text{kg}^{-1}$  with a mean value of 29.01  $\times 10^{-8} \text{ m}^3\text{kg}^{-1}$  in the Refinery\_1 (TSL2) and Refinery\_2 (TSL3) sampling sites, respectively. In Al- Muthanna cement plant\_1 (TSL4) and Al-Muthanna cement plant\_2 (TSL5), the magnetic susceptibilities varied from 16.36 to 38.24  $\times 10^{-8} \text{ m}^3\text{kg}^{-1}$  with a mean values of 31.35  $\times 10^{-8} \text{ m}^3\text{kg}^{-1}$  and from 15.28 to 65.23  $\times 10^{-8} \text{ m}^3\text{kg}^{-1}$  with a mean value of 42.63  $\times 10^{-8} \text{ m}^3\text{kg}^{-1}$ , respectively. Magnetic enhancement could be caused by many factors such as the variation in lithology (lithogenic), processes for soil formation (pedogenesis), and anthropogenic contribution of magnetic signal [9, 7].

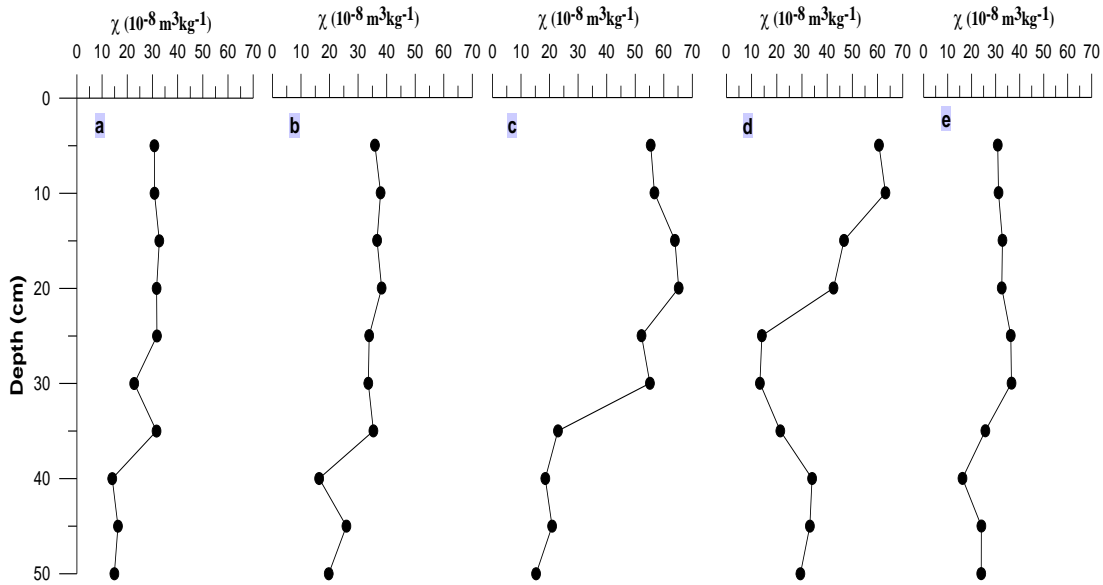


**Figure 2-**Vertical profiles of magnetic susceptibility ( $\chi$ ) versus depth from five sampling sites as follows: (a) Al-Jinoob cement plant (TSL-1); (b) Refinery site (TSL-2); (c) Refinery site (TSL-3); (d) Al-Muthanna cement plant (TSL-4) and (e) Al-Muthanna cement plant (TSL-5).

The high-temperature dependent susceptibility of representative samples is shown in Figure-3A decrease in the cooling curve around the temperature of 580 °C, which is the magnetite curie temperature, can be observed in all samples [10], indicating the presence of magnetite in the samples as the major magnetic mineral. During heating, additional magnetic minerals may be produced because the magnetic susceptibility in the heating curve is greater than in the cooling curve when the temperature is below 500 °C [11].

According to the model presented previously [7], the comparative contribution of fine superparamagnetic particles (SP) to the total assembly of magnetic particles in soils could be asserted by  $\kappa_{fd}\%$ .

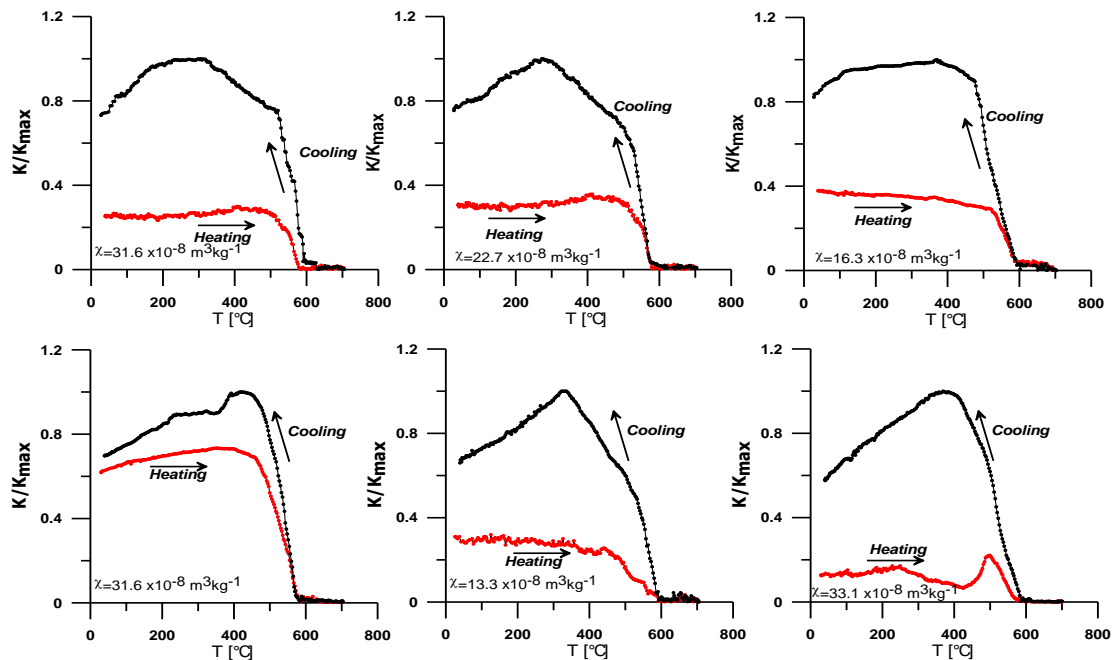


**Figure 3-**High-temperature dependent susceptibility of selected samples; ( $\kappa/\kappa_{max}$  is magnetic susceptibilities versus their maximum values under heating and cooling for each sample).

Our results show low  $\chi_{fd}\%$  values (below 3 %) (Figure-4) in regions of strong magnetic concentration, indicating that the particles are in the grain size range of multi-domain (MD) and pseudo-single domain (PSD). The dominance of strong magnetic minerals indicates that fly ash grains are mainly coarse-grained spheres [12, 13].

The correlation between  $\chi$  and ARM was significant ( $R^2=0.75$ ) (Figure-5); the relatively high correlation indicates the contribution of ferro(i)magnetic minerals in the samples rather than the paramagnetic and superparamagnetic grains [14].

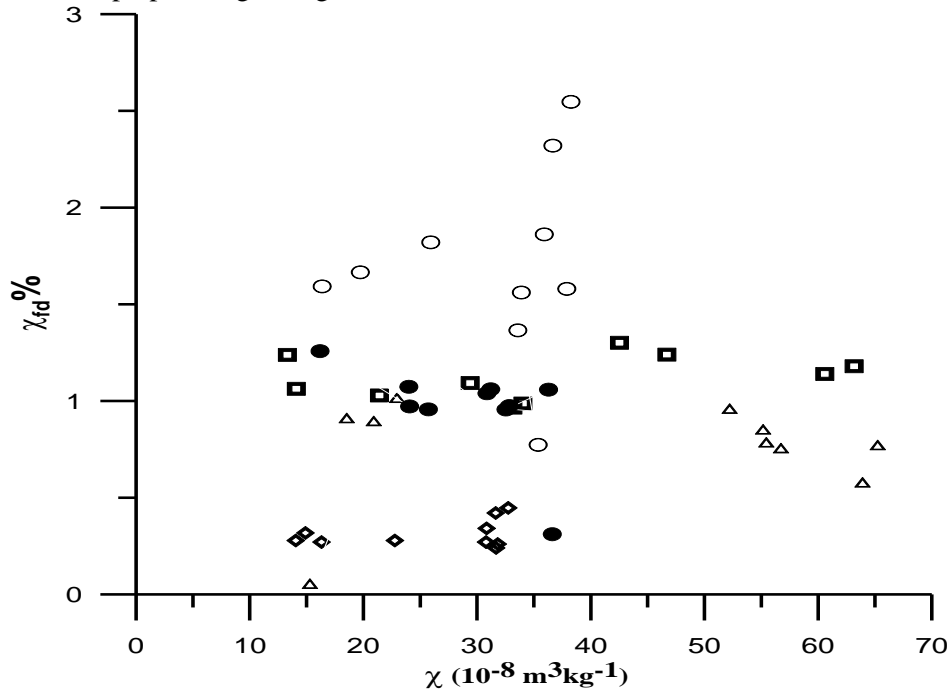


**Figure 4**-Bivariate diagram of  $\chi_{fd}\%$  versus  $\chi$  showing the distribution of magnetic grain sizes in the soils from five sampling sites as follows: (◇) Al-Jinoob cement plant (TSL-1); (△) Refinery site (TSL-2); (□) Refinery site (TSL-3); (●) Al-Muthanna cement plant (TSL-4) and (○) Al-Muthanna cement plant (TSL-5).

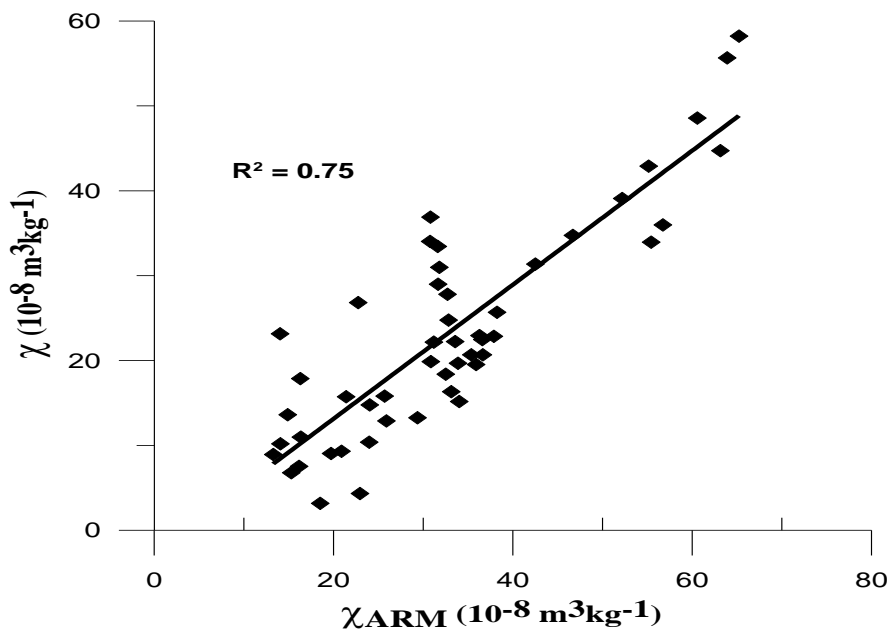


**Figure 5**-Correlation between magnetic susceptibility ( $\chi$ ) and anhysteritic remanent magnetisation (ARM).

To analyse the magnetic components, isothermal remanent magnetisation (IRM) acquisition curves were conducted for selected samples as representative samples (tsl3\_2, tsl3\_4, tsl3\_6, tsl3\_8, tsl3\_10, tsl4\_2, tsl4\_4, tsl4\_6, tsl4\_8, tsl4\_10, tsl5\_2, tsl5\_4, tsl5\_6, tsl5\_8, tsl5\_10) for this study as shown in Figure-6. IRM acquisition curves provide an appropriate way to estimate the proportion of soft and hard magnetic minerals, since soft magnetic minerals such as magnetite can be saturated below 300 mT, whereas hard magnetic minerals such as hematite cannot be saturated even at 1 T [15]. From the measured curves in Figure-6, all the samples show near saturation at 1 T field indicating the dominance of soft magnetic minerals like magnetite and confirming that they are essential in all samples as shown in the thermomagnetic curves (Figure-3)

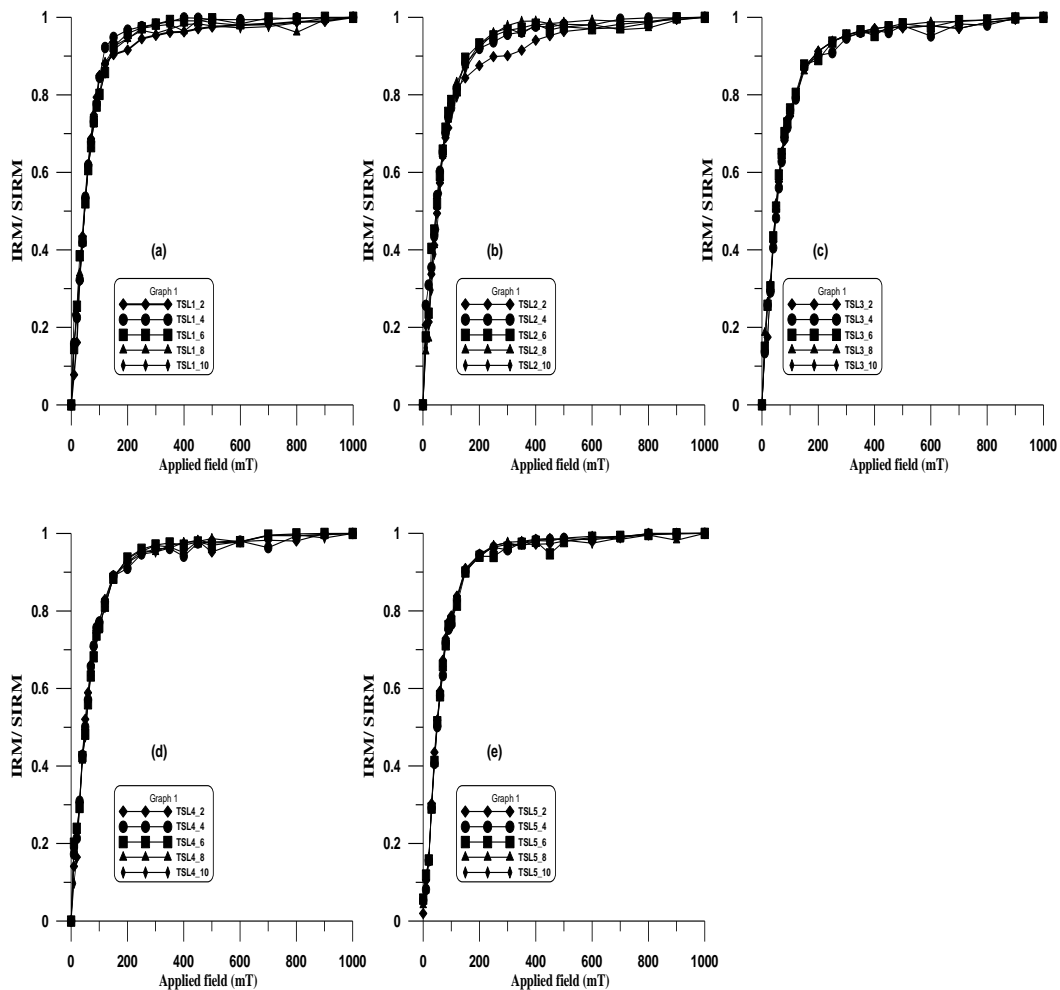


**Figure 6**-Isothermal remanent magnetization (IRM) acquisition curves for selected samples from five sites as follows: (a) Al-Jinoob cement plant (TSL-1); (b) Refinery site (TSL-2); (c) Refinery site (TSL-3); (d) Al-Muthanna cement plant (TSL-4) and (e) Al-Muthanna cement plant (TSL-5).

We further applied cumulative log-Gaussian (CLG) functions which can be used to analyse IRM spectrum [16]. The magnetic component is characterized by its SIRM, the field at which half of the SIRM is reached ( $B/2$ ), and the width of the distribution, expressed through the dispersion parameter DP [17]. Three selected samples were analysed and their summarized results are shown in Table-1. From CLG results, two components can be separated (Figure-7); a low coercivity dominating component (component 1) has  $B/2$  values from 40.2 to 42.4 mT contributing to ~70-80% of the total SIRM, which can be interpreted as magnetite. While the high coercivity component (component 2) has higher  $B/2$  values varying from 120 to 137.3 mT with ~20-30% contribution to the total SIRM (Table-1), which probably represents hematite.

Results of heavy metals of selected samples from five sites show that the highest concentration was for Cr and Ni elements (602.57 and 186.87 ppm, TSL1-5, respectively) (Figure-8). This may be caused by emission of dust from cement plants and its later precipitation into topsoil, because heavy

metals (i.e. Cr, Ni) are involved as raw materials in cement industry. Also, oil industry leads to increase heavy metal concentrations in soil [18, 19].

The levels of heavy metals in the samples varied as follows; Cr (93.04-186.87 ppm), Ni (93.04-186.87 ppm), Cu (12.94-31.87 ppm) and Pb (5.84-13.23 ppm). Cr and Ni levels were above the limits of the World Health Organisations while Cu and Pb were below the limits (Cr 1-5 ppm; Ni 30-75 ppm, Cu 50-140 ppm and Pb 50-300 ppm) [20].

The particle sizes range from 100  $\mu\text{m}$  to 1000  $\mu\text{m}$  according to the grain size measurements using the same samples as for  $\chi$  measurements (Figure-9).

**Table 1**-Log-Gaussian analysis values for the chosen samples shown in Figure-7.

Sample	Component	SIRM (A/m)	Log( $B_{1/2}$ ) (mT)	( $B_{1/2}$ ) (mT)	Contribution (%)
TSL 3-4	1	2982	1.60	40.2	70.4
	2	1251	2.14	137.3	29.6
TSL4-2	1	4435	1.60	40.2	73.5
	2	1597	2.08	120.0	26.5
TSL5-2	1	7189	1.63	42.4	80.1
	2	1784	2.08	120.5	19.9

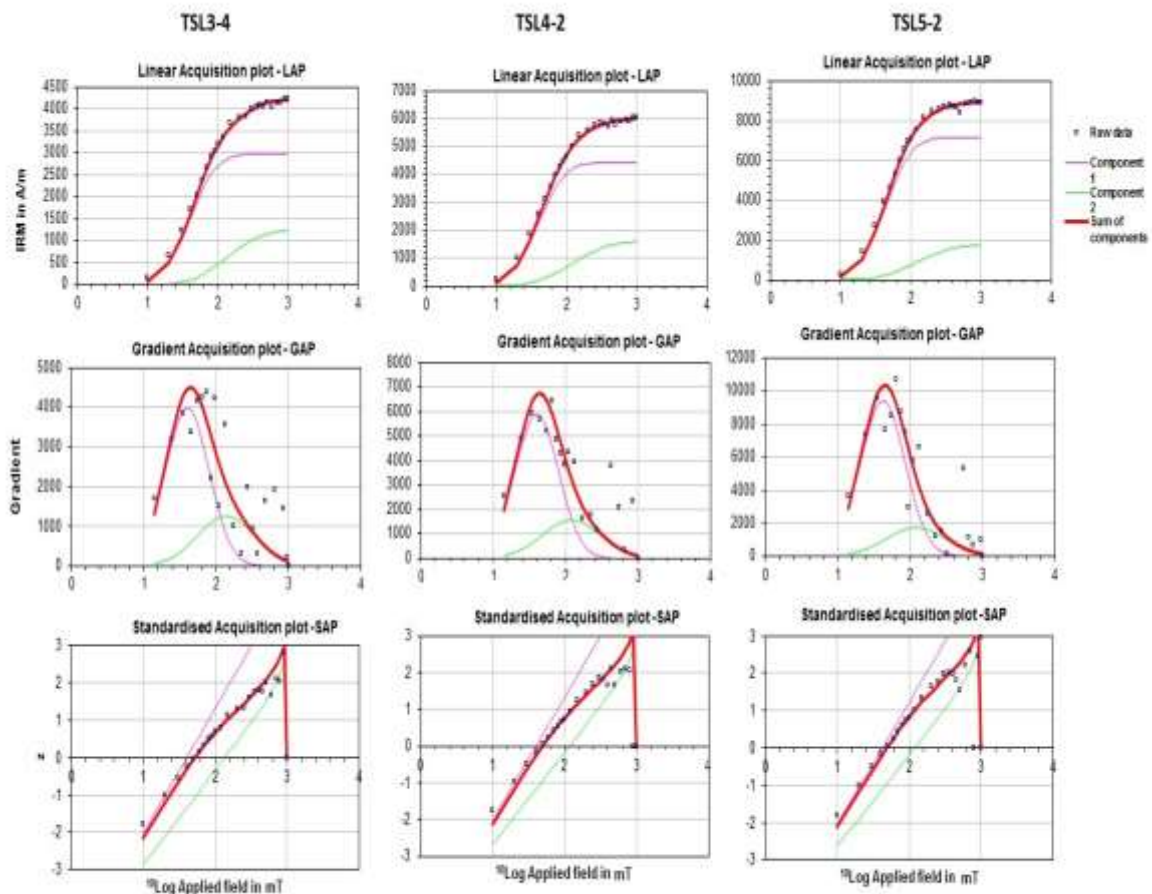


**Figure-7** Quantification of magnetic coercivity components using log-Gaussian analyses of IRM acquisition curves (Kruiver et al., 200). Two components are separated; components 1 with low coercivity which could be magnetite and high coercivity component 2 which could be hematite.



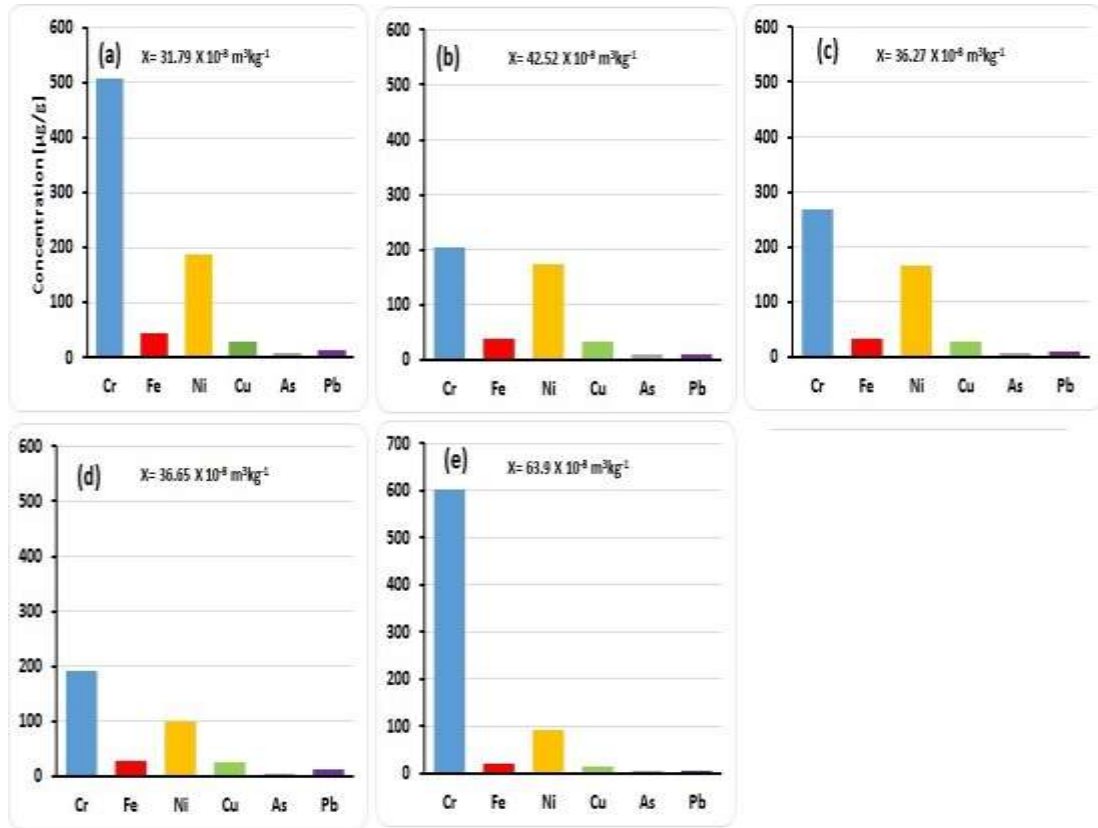


**Figure 8-**Column charts of six heavy metal elements for selected samples (and their  $\chi$  values) from five sites as follows: (a) Al-Jinoob cement plant (TSL-1-5); (b) Refinery site (TSL-2-4); (c) Refinery site (TSL-3-5); (d) Al-Muthanna cement plant (TSL-4-3) and (e) Al-Muthanna cement plant (TSL-5-3).

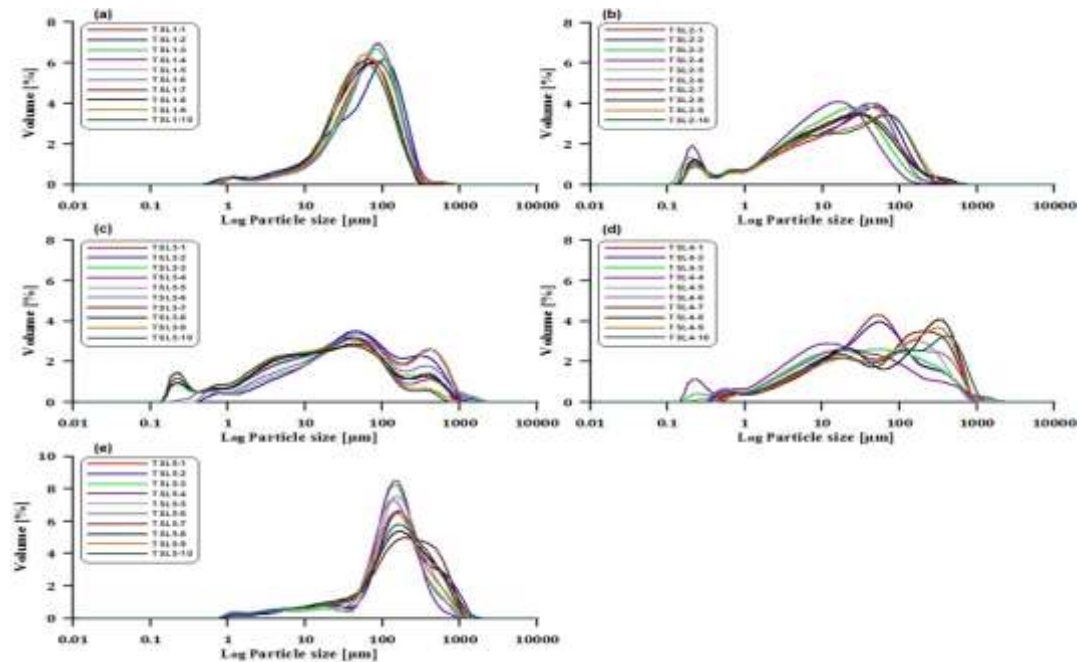


**Figure 9-**Particle size distribution of the same (fifty) samples used for  $\chi$  measurements (measured by Malvern Mastersizer 2000) from five sites as follows: (a) Al-Jinoob cement plant (TSL-1); (b)

Refinery site (TSL2); (c) Refinery site (TSL3); (d) Al-Muthanna cement plant (TSL4) and (e) Al-Muthanna cement plant (TSL5).

### Conclusion

From the results of thermomagnetic analyses (Figure-3) and IRM acquisition (Figure-6), we conclude that magnetite is the dominant phase. According to the results of  $\kappa_{fd}\%$ , the magnetic particles show admixture of multi-domain and pseudo-single domain behaviour. The magnetic enhancement could be due to pedogenic particles in natural soil, causing the positive correlation between  $\chi$  and ARM (Figure-5). We also can conclude that the soils from the five studied locations are contaminated by industrial materials due to the fact that all samples have higher  $\chi$  values but lower  $\kappa_{fd}\%$  values [21].

### Acknowledgement

I would like to thank Erwin Appel from university of Tübingen (Germany), Department of Geosciences for providing access to the magnetic laboratories. I'm also grateful to Qusay Abeed from Halliburton for his review and feedback efforts.

### References

1. El Baghdadi M., Jakani K., Barakat A. And Bay Y. **2011**. Magnetic susceptibility and heavy metal contamination in agricultural soil. *Journal of materials and environmental science (S1)*: 513-519. ISSN: 2028-2508.
2. Magiera, T., Gołuchowska B. and Jabłońska M. **2013**. Technogenic Magnetic Particles in Alkaline Dusts from Power and Cement Plants. *Water, Air, & Soil Pollution*, **224**: 1389, DOI 10.1007/s11270-012-1389-9.
3. Ameen N., Rasheed L., Khwedim K. **2019**. Evaluation of Heavy Metal Accumulation in Sawa Lake Sediments, Southern Iraq using Magnetic Study. *Iraqi Journal of Science*, [S.l.], **60**: 781-791.
4. Canbay M, Aydin A. and Kurtulus C. **2010**. Magnetic susceptibility and heavy-metal contamination in topsoils along the Izmit Gulf coastal area and IZAYTAS (Turkey). *Journal of applied geophysics*, **70**: 46–57.
5. Peng L., Xiao-Ke1 Q., Xin-Wen X., Xu-Bin L. and Yu-Fang S., **2010**. Magnetic properties of street dust: a case in xi'an city, shaanxi province, china. *Chinese journal of geophysics*, **53**(1): 113-120.
6. Al-Rawi F.R., Al-Badri A.S. and Rezkalla J.S. **1989**. Application of microgravimetric survey in Samawa salt deposit, Iraq. *Geophysics*, **54**: 440-444. DOI: <https://doi.org/10.1190/1.1442669>.
7. Dearing, J.A., Hay, K.L., Baban, S.M.J., Huddleston, A.S., Wellington, E.M.H., Loveland, P.J., **1996**. Magnetic susceptibility of soil: an evaluation of conflicting theories using a national data set. *Geophysical. Journal International*, **127**: 728– 734.
8. Bloemendal J., King J.W., Hall F.R. and Doh S.J. **1992**. Rock magnetism of late Neogene and Pleistocene deep-sea sediments: relations to sediment source, diagenetic process, and sediment lithology. *Journal of Geophysical Research*, **97**: 4361-4375.
9. Newson M., **1988**. *Environmental magnetism by Roy \_Thompson and Frank Oldfield*, **13**, Allen and Unwin, London, UK.
10. Thompson, R. & Oldfield, F., **1986**. *Environmental Magnetism*, Allen & Unwin, London.
11. Hu, S.Y., Duan, X. M., Shen, M.J., **2008**. Magnetic response to atmospheric heavy metal pollution recorded by dust-loaded leaves in Shougang industrial area, western Beijing. *Chinese Science Bulletin*, **53**(10): 1555–1564. doi: 10.1007/s11434-008-0140-9.
12. Flanders, P., **1994**. Collection, measurement, and analysis of airborne magnetic particulates from pollution in the environment. *Journal of Applied Physics*, **75**: 5931-5936.
13. Jordanova, D., Jordanova, N., Petrov, P., **2014**. Magnetic susceptibility of road deposited sediments at a 459 national scale-relation to population size and urban pollution. *Environmental Pollution*, **189**: 239-251.
14. Yin Gang, Hu Shouyun, Cao Liwan, Roesler Wolfgang, Appel Erwin, **2013**. Magnetic properties of tree leaves and their significance in atmospheric particle pollution in Linfen City, China. *Chinese Geographical Science*, **23**(1): 59–72. doi: 10.1007/s11769-013-0588-7.
15. Ma M.M, Hu S.Y., Lin H., Cao L.W., Wang L.S., **2014**. Magnetic responses to traffic related contamination recorded by backfills: A case study from Tongling City, China. *Journal of applied geophysics*. **107**: 119-128.

16. Robertson D.J. and. France D.E., **1994**. Discrimination of remanence-carrying minerals in mixtures, using isothermal remanent magnetisation acquisition curves. *Physics of the Earth and Planetary Interiors*. **82**: 223-234.
17. Kruiver, P.P., and H. F. Passier, **2001**. Coercivity analysis of magnetic phases in sapropel S1 related to variations in redox conditions, including an investigation of the S ratio, *Geochemistry, Geophysics. Geosystem.*, vol. **2**.
18. Ešťoková, A., Palaščáková, L., Singovszká, E., & Holub, M., **2012**. Analysis of the chromium concentrations in cement materials. *Procedia Engineering*, **42**: 123–130. <https://doi.org/10.1016/j.proeng.2012.07.402>
19. Sharma, D. K., & Katyal, N. K. **2014**. Study of total chromium and water soluble chromium in Indian cement samples. *International Journal of Advancements in Research & Technology*, **3**(2) February-2014. ISSN 2278-7763.
20. World health organization (WHO), **2003**. *Regional Office for the Eastern Mediterranean, Environmental health activities*, Amman, Jordan, wastewater use in agriculture, A Handbook guide. (In arabic).
21. Blundell, A., Hannam, J.A., Dearing, J.A. and Boyle, J.F. **2009**. Detecting atmospheric pollution in surface soils using magnetic measurements: a reappraisal using an England and Wales database. *Environmental Pollution*, **157**: 2878-2890. (doi:10.1016/j.envpol.2009.02.031).